CLEO-PR & OECC/PS 2013

The 10th Conference on Lasers and Electro-Optics Pacific Rim, and
The 18th OptoElectronics and Communications Conference / Photonics in Switching 2013

News & Information

NEW	2013/05/27	Post Deadline Paper(PDP) Submission Started.
	2013/05/24	Student Travel Grant Page Opened.
	2013/05/21	Program has been uploaded.
	2013/05/07	Student Travel Grant Page will be available soon.
	2013/04/30	Student Travel Grant Page will be available May 8, 2013.
	2013/04/24	Accommodation & Tours Page Opened.

Important Dates

Paper Submission
Start : December 10, 2012
End : ~~February 4, 2013~~ **February 22, 2013**
(Japan Standard Time, UTC +9)

Acceptance Notification ~~End of March, 2013~~ **Beginning of April, 2013**

Early Registration
Start : March 1, 2013 End : May 31, 2013

Post Deadline Paper(PDP) Submission
Start : ~~May 20, 2013~~ End : June 20, 2013
May 27, 2013 (Japan Standard Time, UTC +9)

CLEO-PR 2013
Cosponsored by:
IEICE CS IEICE ES

The Japan Society of Applied Physics

OECC/PS 2013
Cosponsored by:
IEICE CS IEICE ES

TuPL-8
Phenomenon of Hygroscopicity in a Fiber Fabry-Pérot Interferometer with an Absorbent Polymer Cavity

Chien-Chih Liu[1], Yan-Wun You[1], Lih-Gen Sheu[2], Jui-Ming Hsu[1] and Cheng-Ling Lee[1]

[1] Dept. of Electro-Optical Engineering, National United Univ., Miaoli, Taiwan, [2] Dept. of Electro-Optical Engineering, Vanung Univ., Taoyuan, Taiwan

We experimentally measure the hygroscopicity of liquid by using ultracompact fiber Fabry-Pérot interferometers (FFPIs) with an absorbent polymer-microcavity in a hollowcore-fiber. Experimental results of Adsorption and desorption behaviors show a hysteresis phenomenon during the processes.

TuPL-9
Optical Waveguide Resonator for Refractive Index Change Sensor Using Arrayed Waveguide with Grating to Couple Light Beam

H. Irikawa[1], H. Okayama[1,2], N. Fujiwara[1], T. Ooka[1] and H. Nakajima[1]

[1] Waseda Univ., Shinjyuku, Japan, [2] Oki Electric Industry, Saitama, Japan

We report waveguide optical sensor using wire waveguide array. Grating coupler is used to couple waveguide modes with input and output light beam. The cavity is formed by new reflector structure or ring waveguide.

TuPL-10
Dispersion Model for AWG-Based Filters Under the Influence of Random Phase Errors

Koichi Maru

Dept. of Electronics and Information Engineering, Faculty of Engineering, Kagawa Univ., Kagawa, Japan

A statistical model of chromatic dispersion (CD) in filters using arrayed waveguide gratings (AWGs) with random phase errors is proposed. The average and variance of CD in the passband can be calculated using simple expressions.

TuPL-11
Variable Time Delay Experiments in Serially Cascaded Ring Resonator All-Pass Filters

Jaeseong Kim, Yoonyoung Ko, Hyosuk Kim, and Youngchul Chung

Dept. of Electronics and Communications Engineering, Kwangwoon Univ., Seoul, Republic of Korea

Serially cascaded single-ring resonator APF's (All-Pass Filters) are implemented in polymer waveguide for the realization of variable optical delay device. When all of 8 rings are resonannt, the delay is measured to be about 160ps.

TuPL-12
Waveguide Optical Triplexer with Cascaded Multi-Mode Interference Couplers

Ryosuke Yokote, Yuta Kojima, Hideki Yokoi

Dept. of Electronic Engineering, Shibaura Inst. of Technology, Tokyo, Japan

An optical triplexer with cascaded multi-mode interference couplers was proposed in an optical access system. The optical triplexer on a silicon-on-insulator substrate was designed by beam propagation method. The optical triplexer was fabricated and evaluated.

TuPL-13
Design, Fabrication and Properties of Optical Large Core Polymer Planar 1x2 Splitter

V. Prajzler, R. Mastera, and V. Jerabek

Dept. of Microelectronics, Faculty of Electrical Engineering, Czech Technical Univ. in Prague, Prague, Czech Republic

We report about properties of multimode polymer 1x2 optical planar splitter. The splitters have the insertion loss around 6.96 dB for a structure comprising POF fibers and 4.38 dB (650 nm) with FG910LEC fibers.

TuPL-14
Quasi-LP21 Mode Converter by Using Simple Step-Core Structure

Yutaka Chaen [1], Zhao Zhao[1], Yuuta Satou[2] and Kiichi Hamamoto[1]

[1] Interdisciplinary Graduate School of Engineering Science, Kyushu Univ., Japan, [2] Faculty of Engineering, Kyushu Univ., Japan

We propose multi-mode interference (MMI) based multi-mode converter for future spatial multi-mode multiplexing transmission. The designed MMI multi-mode converter could convert 0th mode up to LP21 mode.

TuPL-15
Fast Mode Splitting in Engineered Multimode Waveguides

Shuo-Yen Tseng, Chi-Shung Yeih, and Kai-Hsun Chien

Dept. of Photonics, National Cheng Kung Univ., Tainan, Taiwan

We propose fast mode splitting in multimode waveguides based on Lewis-Riesenfeld invariant theory. Mode converters are designed using computer-generated planar holograms to implement the coupling coefficients obtained from the dynamical invariants.

TuPL-16
SESAM-Based Ring-cavity All-normal-dispersion Tunable Ytterbium Mode-locked Fiber Laser

Doudou Gou[1], Sigang Yang[1], Feifei Yin[2], Lei Zhang[1], Fangjian Xing[1], Hongwei Chen[1], Minghua Chen[1], and Shizhong Xie[1]

[1] Tsinghua National Laboratory for Information Science and Technology (TNList) Dept. of Electronic Engineering, Tsinghua Univ., Beijing, P.R.China, [2] State Key Laboratory of Information Photonics & Optical Communications (Beijing Univ. of Posts and Telecommunications), Beijing, China

Based on a SEMSAM, an all-normal-dispersion ring cavity, tunable (1033-1069nm), Ytterbium-doped passively mode-locked fiber laser is demonstrated (repetition rate: 25.4MHz). The output pulse is compressed from 34.85ps to 15.45ps by using single-channel grating pairs.

TuPL-17
Characteristics of Glass Phosphor with Ce^{3+}:YAG Particle Coated SiO_2 by Sol-Gel Method

Wei-Chih Cheng[1], Chun-Chin Tsai[1,2], Shi-Sheng Hu[1], Jin-Kai Chang[1], Yu-Lun Lin[2], Li-Yin Chen[1], Yi-Chung Huang[1], Yi-Cheng Hsu[3], and Wood-Hi Cheng[1], IEEE Fellow

[1] Dept. of Photonics, National Sun Yat-sen Univ., Kaohsiung, Taiwan, [2] Dept. of Optoelectronic Engineering, Far East Univ., Tainan, Taiwan, [3] Dept. of Biomechatronics Engineering, National Pingtung Univ. of Science and Technology, Taiwan

The characteristics of sol-gel glass phosphor have been investigated. The sol-gel glass phosphor showed 1.5% and 9.5% more efficient in quantum efficiency and luminous efficiency respectively than sintered glass phosphor.

TuPL-18
Formation of Holographic Memory by Recording of Multi-context in Liquid Crystal Composites

Akifumi Ogiwara[1], Hikaru Maekawa[1], Minoru Watanabe[2], and Retsu Moriwaki[2]

[1] Dept. of Electronic Engineering, Kobe City College of Technology, Kobe, Japan, [2] Faculty of Engineering, Dept. of Electrical and Electronic Engineering, Shizuoka Univ., Hamamatsu, Japan

A holographic polymer-dispersed liquid crystal (HPDLC) memory to record multi-context information for an optically reconfigurable gate array is formed by a successive laser exposure in LC composites.

TuPL-19
Ultracompact Narrowband Three-Dimensional Hybrid Plasmonic Waveguide Bragg Grating

Yin-Jung Chang and Chun-Yu Chen

Dept. of Optics and Photonics, National Central Univ., R.O.C. (Taiwan)

A novel ultracompact three-dimensional waveguide plasmonic Bragg grating in metal/multi-insulator/metal configuration is investigated. Narrowband characteristics (FWHM bandwidth: 10.8 nm, extinction ratio: 11.91 dB) are numerically demonstrated within a footprint of <17 um^2.

TuPL-20
G-s_0 Mode Converter for Nano Plasmonic Integrated Circuits

Dong Hun Lee[1], Jung-Han Son[1], Hae-Ryeong Park[2], Min-su Kim[3] and Myung-Hyun Lee[1]

[1] School of Information and Communications Engineering, Sungkyunkwan Univ., Suwon, Korea, [2] CAE Group, LCD R&D Center, LCD Business, Samsung Electronics Co. Ltd., Gyeonggi-Do, Korea, [3] Electronics & Telecommunications Research Inst., Daejeon, Korea

We propose a G-s_0 mode-size converter (MC) from the Ss_0 mode to the G-s_0 mode at a wavelength of 1.55 um.

TuPM-1
High-Extinction Si Photonic-Crystal Optical Modulators At 10 Gb/s

Naoya Yazawa, Hong C. Nguyen, Satoshi Hashimoto, Toshihiko Baba

Dept. of Electrical and Computer Engineering, Yokohama National Univ. Tokiwadai, Yokohama, Japan

We optimized the 10 Gb/s operation in Si photonic crystal optical modulators with 50-200 μm phase-shifter lengths. By incorporating additional phase-tuners, we obtained over 10 dB extinction ratio and error-free operation.

TuPM-2
GHz Response of MSM InGaAs Photodetector on Si Substrate by BCB Bonding

Kazuaki MAEKITA, Takeo MARUYAMA, and Koichi IIYAMA

Graduate School of Natural Science and Technology, Kanazawa Univ., Ishikawa, JAPAN

We fabricated an InGaAs MSM-PD bonded on Si substrate by BCB bonding. The responsivity of 0.035A/W and the dark current of 29nA were obtained. The bandwidth of 3GHz was obtained at 10V.

TuPM-3
Selectable Heterogeneous Integrated III-V /SOI Single Mode Laser Based on Vernier Effect

Zhao Huang, Yi Wang

Wuhan National Laboratory for Optoelectronics, Huazhong Univ. of Science and Technology, Wuhan, China

A novel heterogeneous integrated III-V/SOI single mode laser is proposed. Owing to vernier effect between Fabry-Perot resonator and split silicon racetrack resonator, single longitudinal mode can be obtained and selected by thermally tuned silicon waveguide.

TuPM-4
Luminescence of $Er_xY_{2-x}SiO_5$ in Si Slot Waveguide Structures

Y. Terada, S. Ban, Z. I. Bin Zulkefli, T. Nakajima, T. Kimura, and H. Isshiki

Dept. of Engineering Science, The Univ. of Electro-Communications, Tokyo, Japan

Strong optical confinement to the low-index slot, such as $Er_xY_{2-x}SiO_5$, is expected for TM mode in Si slot waveguide. We have fabricated slab Si-slot waveguides with Er_2SiO_5 slot layers.

TuPM-5
An Equivalent Circuit with a Noise Source for 850-nm Si Avalanche Photodetector and Optimal Design of Si OEIC Receiver

Jin-Sung Youn[1], Myung-Jae Lee[1], Kang-Yeob Park[1], Holger Rücker[2], and Woo-Young Choi[1]

[1] Dept. of Electrical and Electronic Engineering, Yonsei Univ., Seoul, Korea, [2] IHP, Frankfurt (Oder), Germany

Equivalent circuit model including noise current source is developed for 850-nm Si avalanche photodetector (APD). The measured APD signal-to-noise characteristics are modeled with circuit parameters and used for realizing the optimal 12.5-Gbps Si OEIC receiver.

TuPM-6
Enhanced Dispersive and Nonlinear Properties of Coupled Ring Resonators by Using an Embedded Microrings Configuration

Xiaoyan Zhou[1], Lin Zhang[2], Andrea M. Armani[3], Hao Zhang[1], and Wei Pang[1]

[1] State Key Laboratory of Precision Measuring Technology and Instruments, Tianjin Univ., Tianjin, China, [2] Microphotonics Center and Dept. of Materials Science and Engineering, Massachusetts Inst. of Technology, Cambridge, USA, [3] Mork Family Dept. of Chemical Engineering and Materials Science, Univ. of Southern California, Los Angeles, USA

We study both the intensity and phase responses in embedded rings operated in analogy to electromagnetically induced transparency. Different phase regimes have been identified, which correspond to different optical nonlinear enhancement characteristics.

TuPM-7
Systematic Comparison of FWM Conversion Efficiency in Silicon Waveguides and MRRs

Meng Xiong[1,2], Yunhong Ding[2], Haiyan Ou[2], Christophe Peucheret[2], and Xinliang Zhang[1]

[1] Wuhan National Laboratory for Optoelectronics, School of Optoelectronics Science and Engineering, Huazhong Univ. of Science and Technology, Wuhan, Hubei, People's Republic of China, [2] Dept. of Photonics Engineering, Technical Univ. of Denmark, Lyngby, Denmark

Wavelength conversion based on four-wave mixing is theoretically compared in silicon micro-ring resonators and nanowires under the effect of nonlinear loss. The impact of the bus waveguide length and MRR position are also quantified.

An Equivalent Circuit with a Noise Source for 850-nm Si Avalanche Photodetector and Optimal Design of Si OEIC Receiver

Jin-Sung Youn*, Myung-Jae Lee*, Kang-Yeob Park*, Holger Rücker**, and Woo-Young Choi*

* Department of Electrical and Electronic Engineering, Yonsei University, Seoul, Korea
** IHP, lm Technologiepark 25, 15236 Frankfurt (Oder), Germany
wchoi@yonsei.ac.kr

Abstract

Equivalent circuit model including noise current source is developed for 850-nm Si avalanche photodetector (APD). The measured APD signal-to-noise characteristics are modeled with circuit parameters and used for realizing the optimal 12.5-Gbps Si OEIC receiver.

I. Introduction

For short-reach optical interconnect applications, high-performance optoelectronic integrated circuit (OEIC) receivers are highly desirable. Monolithic integration of Si electronics with Si photodetector provides performance enhancement as well as cost effectiveness [1]. Several Si OEIC receivers have been reported [2], [3]. We have demonstrated OEIC receivers with on-chip Si avalanche photodetector (APD) in standard Si technology [4], [5]. In order to optimize OEIC receiver design and, eventually, implement OEIC receiver as a sub-block of much larger Si electronic systems, it is essential to develop design methodology in which the optical devices are co-designed and co-simulated with electronic circuits on Si platform. For this goal, we have previously reported an equivalent circuit model of Si APD [6] that allows unified circuit-level simulation for the entire OEIC receiver.

In this paper, we further enhance the model by adding the APD noise characteristics. This is an important task as APDs provide much enhanced noises as well as signals. APD noise characteristics are measured for different reverse bias voltages, and the results are modeled by a noise current source. This allows us design optimization of the entire OEIC receiver. A 12.5-Gbps 850-nm OEIC receiver is successfully realized with such design optimization.

II. Equivalent Circuit Model For Si APD

Fig. 1 shows a simplified block diagram of Si OEIC receiver. An APD equivalent circuit model is composed of parasitic RLC components and a signal current source as well as a noise current source. APD noise characteristics can be modeled with Gaussian distribution in the case of Si APD having small excess noise factors [7]. The $I_{s,pp,APD}$ represents peak-to-peak signal current, and $I_{n,rms,APD}$ represents root mean square (rms) noise current. Fig. 2 shows the measured $I_{s,pp,APD}$ and $I_{n,rms,APD}$ of our APD as a function of reverse bias voltage (V_R) at

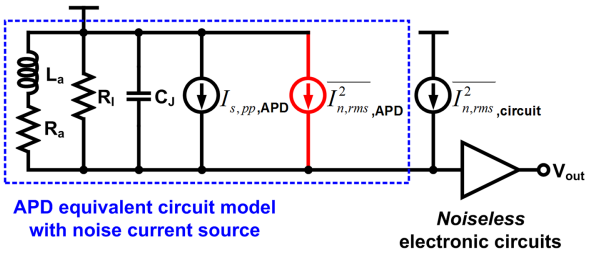

Fig. 1. Simplified block diagram of Si OEIC receiver.

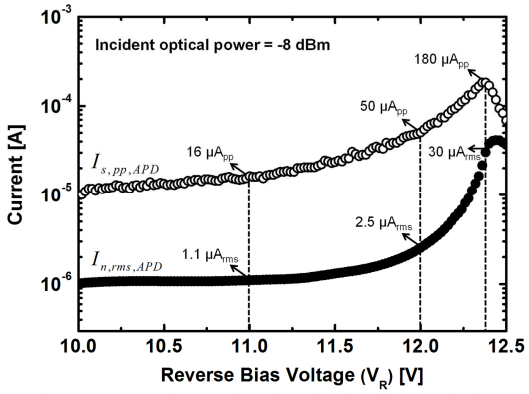

Fig. 2. Measured APD signal and noise characteristics.

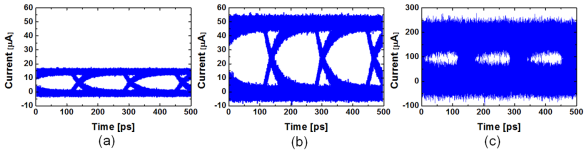

Fig. 3. Simulated eye diagrams with different reverse bias voltages (V_R) of (a) 11.0 V, (b) 12.0 V, and (c) 12.4 V.

incident optical power of -8 dBm. For signal measurement, 1-GHz sinusoidal signal is modulated by using an 850-nm laser diode and an external electro-optic modulator. The modulated light is transmitted through multimode fiber, and injected into the APD using a lensed fiber. For noise measurement, noise power spectral density at 1 GHz is measured without any RF signal applied to the modulator. With the increasing V_R, signal current is enhanced due to avalanche gain, and noise current is also increased due to avalanche noise. Fig. 3 show the simulated eye diagrams of APD output currents at three different bias voltages of 11.0, 12.0, and 12.4 V, respectively. This simulation is done with Spectre circuit simulator in Cadence by adding the APD noise model with Verilog-A. As shown in Fig. 3, signal amplitude is increased with the increasing V_R, however, signal quality

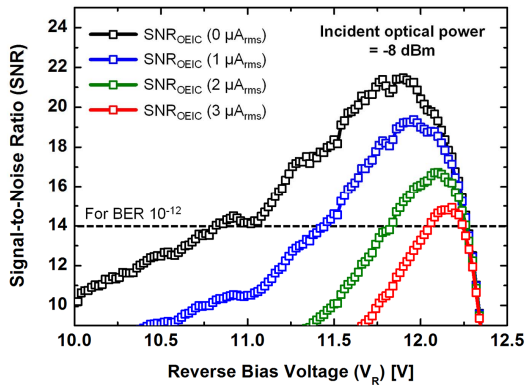

Fig. 4. Estimated signal-to-noise ratio of APD and OEIC receiver.

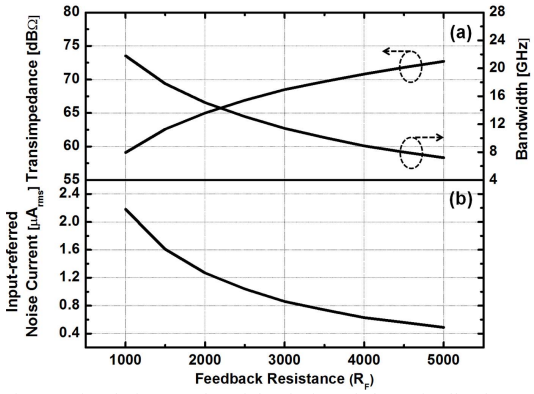

Fig. 5. Simulation results of the designed shunt-feedback TIA.

can be degraded due to increased avalanche noise.

III. OEIC Receiver Design Optimization

As shown in Fig. 1, the noise characteristics of the entire electronic circuit can be modeled with a circuit noise current source with $I_{n,rms,circuit}$ represents rms input-referred noise current of electronic circuits. Then, the signal-to-noise ratio (SNR) of the OEIC receiver is given as:

$$SNR_{OEIC}(V_R) = \frac{I_{s,pp,APD}(V_R)}{\sqrt{\overline{I^2_{n,rms,APD}}(V_R) + \overline{I^2_{n,rms,circuit}}}}. \quad (1)$$

Fig. 4 shows the estimated SNR_{OEIC} for different $I_{n,rms,circuit}$ of 0, 1, 2, and 3 μA_{rms}. To achieve a bit-error rate (BER) less than 10^{-12}, SNR of about 14 is required, and therefore, $I_{n,rms,circuit}$ should be minimized to less than 1 μA_{rms}. This figure also shows that the APD bias should be carefully controlled in order to achieve the optimal OEIC receiver SNR.

In order to achieve high gain and low-noise transimpedance amplifier (TIA), the shunt-feedback architecture is used [8]. Fig. 5 shows simulation results of our TIA as a function of feedback resistance (R_F). In order to achieve $I_{n,rms,circuit}$ less than 1 μA_{rms}, R_F larger than 2.5 kΩ is needed. We used R_F of 3 kΩ, which gives $I_{n,rms,circuit}$ of 0.86 μA_{rms}, transimpedance of 68.5 dBΩ, and bandwidth of 11.4 GHz in Spectre simulation.

IV. Measurement Results

With above mentioned design optimization, we realized an OEIC receiver with monolithically integrated

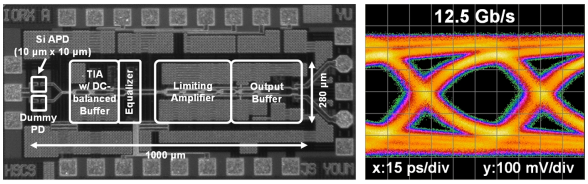

Fig. 6. (a) Chip photograph and (b) Measured eye diagram.

Si APDs in standard 0.25-μm SiGe BiCMOS technology [5]. With the fabricated OEIC receiver, 12.5-Gbps broadband optical data is successfully detected. Fig. 6(a) and (b) show chip photograph and measured 12.5-Gbps eye diagram, respectively. To the best of our knowledge, our OEIC receiver achieves the highest data rate among previously reported Si OEIC receivers.

V. Conclusions

We report an 850-nm Si APD equivalent circuit model including the noise current source and the process of design optimization of Si OEIC receiver. With the fabricated OEIC receiver, we successfully achieve 12.5-Gbps broadband optical data transmission with BER less than 10^{-12}.

Acknowledgment

This work was supported by the National Research Foundation of Korea (NRF) grant funded by the Korea government (MEST) [2012R1A2A1A01009233]. The authors are thankful to IDEC for EDA software support.

References

[1] T. K. Woodward and A. V. Krishnamoorthy, "1-Gb/s integrated optical detectors and receivers in commercial CMOS technologies," *IEEE J. Sel. Topics Quantum Electron.*, vol. 5, no. 2, pp. 146-156, Mar.-Apr., 1999.

[2] S. Radovanovic, A.-J. Annema, and B. Nauta, "3-Gb/s optical detector in standard CMOS for 850-nm optical communication," *IEEE J. Solid-State Circuits,* vol. 40, no. 8, pp. 1706-1717, Aug., 2005.

[3] S.-H. Huang, W.-Z. Chen, Y.-W. Chang, and Y.-T, Huang, "A 10-Gb/s OEIC with meshed spatially-modulated photo detector in 0.18-μm CMOS technology," *IEEE J. Solid-State Circuits*, vol. 46, no. 5, pp. 1158-1169, May, 2011.

[4] J.-S. Youn, M.-J. Lee, K.-Y. Park, and W.-Y. Choi, "10-Gb/s 850-nm CMOS OEIC receiver with a silicon avalanche photodetector," *IEEE J. Quantum Electron.*, vol. 48, no. 2, pp. 229-236, Feb., 2012.

[5] J.-S. Youn, M.-J. Lee, K.-Y. Park, H. Rücker, and W.-Y. Choi, "An integrated 12.5-Gb/s optoelectronic receiver with a silicon avalanche photodetector in standard SiGe BiCMOS technology," *Opt. Express*, vol. 20, no. 27, pp. 28153-28162, Dec., 2012.

[6] M.-J. Lee, H.-S. Kang, and W.-Y. Choi, "Equivalent circuit model for Si avalanche photodetectors fabricated in standard CMOS process," *IEEE Electron Device Lett.*, vol. 29, no. 10, pp. 1115-1117, Oct., 2008.

[7] P. P. Webb, R. J. McIntyre, and J. Conradi, "Properties of avalanche photodiodes," *RCA Review,* vol. 35, pp. 234-278, June, 1974.

[8] E. Säckinger, "The transimpedance limit," *IEEE Trans. Circuits Syst. I, Reg. Papers*, vol. 57, no. 8, pp. 1848-1856, Aug. 2010.